ministerie van verkeer en waterstaat

koninklijk nederlands meteorologisch instituut

A scintillation experiment over a forest

W. Kohsiek

Scientific reports; WR-92-04
Wetenschappelijke rapporten; WR-92-04

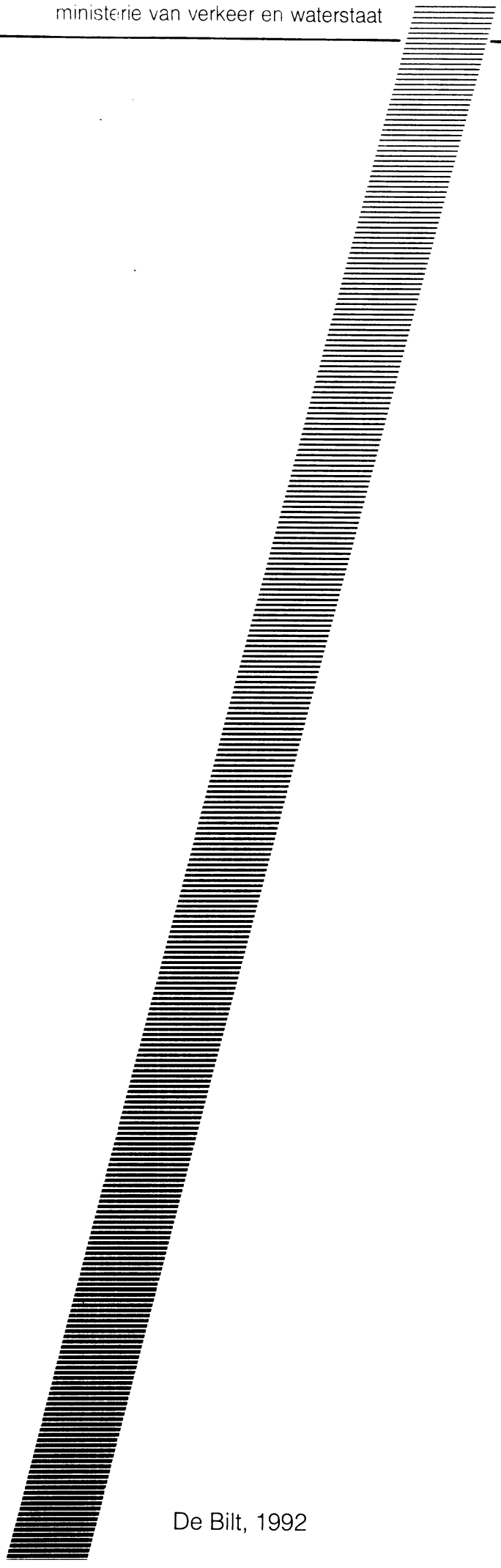

De Bilt, 1992

de bilt 1991 publicationnummer: scientific reports=
wetenschappelijke rapporten: WR-92-04

p.o.box 201
3730 AE de bilt
wilhelminalaan 10
telefoon +31 30 206911
telex 47096
fax +31 30 201364

U.D.C.: 551.551.8
551.584.41
551.593.12
(492)

ISSN: 0169-1651

ISBN: 90-369-2023-X

A SCINTILLATION EXPERIMENT OVER A FOREST

W. Kohsiek
Royal Netherlands Meteorological Institute (KNMI),
De Bilt, The Netherlands

Abstract

Scintillation measurements were carried out on a path of 1640 m over an inhomogeneous forest. The objective was to study the relation between locally observed heat fluxes over a Douglas fir stand, and area average heat fluxes derived from the scintillometer. It was found that the application of the scintillation technique was hampered by two factors: uncertainty regarding the scaling of the dimensionless temperature structure parameter at near-neutral atmospheric stability, and second, uncertainty regarding the effective height of the optical path over the forest. Because of these limitations, no definite answer on the representativeness of the local measurements could be given.

1. Introduction

In this report scintillation measurements over a forest will be discussed. The measurements were carried out as part of a comprehensive measuring campaign at a location near the town of Garderen. The prime objective of the campaign was to study the dry deposition of ammonia in the forest, and its effect on the vitality of the trees. In the campaign several groups with different disciplines participated. The task of the KNMI was to assess the exchange coefficient for the vertical transport of air pollutants. To this purpose, a 36 m high tower was erected in a lot with Douglas fir, with sensors for wind speed, temperature, humidity, fluxes of heat, momentum and water vapour, radiation etc. More details are given by Bosveld et al., 1992. The purpose of the scintillometer measurement was to compare area averaged heat fluxes with the tower measurements of the heat flux. From the comparison, a judgement should be made of the representativeness of the tower measurements.

2. The scintillometer and structure parameters

An instrument with 15 cm aperture transmitter and receiver was used, with a light emitting diode (0,94 μm) as a light source (Kohsiek, 1987). The transmitter was positioned on a former fire tower at the village of Drie, at a height of 31.5 m above the local surface. The receiver was mounted at 36 m above the forest floor on top of the KNMI tower near Garderen, and 1640 m from the transmitter. The forest floor between the two locations is not level, and the forest itself inhomogeneous: different species, different tree heights. Figures 1 and 2 give a picture of the situation. In deriving the sensible heat flux from the refractive index structure parameter (the quantity

directly measured by the scintillometer), the height above the surface enters. For instance, if the condition of free convection applies,

$$Q_o = 0.55\, z \left(\frac{g}{T}\right)^{1/2} \left(C_T^2\right)^{3/4}, \qquad (1)$$

where Q_o is the temperature flux, z the height above the surface, g the acceleration of gravity, and T the air temperature in K (Kohsiek, 1982). C_T^2 is the temperature structure parameter and is linearly related to C_n^2, the refractive index structure parameter; this will be discussed below. So, in case of free convection, the calculated heat flux is proportional to the height above the surface. Now a practical problem enters. Whereas it is relatively simple to define the height over a comparatively short vegetation, it is not so straightforward if the optical path runs relatively close to the treetops. From the work of Bosveld (1991) it is concluded that an acceptable displacement height is 2/3 times the height of the trees. Applying this rule, it was found that the middle section of the optical path, which is most heavily weighted by the scintillometer, is at about 23 m above the displacement height. Following the same rule, the in-situ measurements of C_T^2 (to be discussed shortly below) were at 18 m above the vegetation. Where relevant, the effect of the height difference on the interpretation of the results will be noted. In-situ measurements of C_T^2 were done with a high response speed Platinum wire thermometer mounted close to a Lyman-alpha hygrometer. Using the time delay approach (Kohsiek, 1982), measurements of C_T^2, C_{TQ} and C_Q^2 were obtained. From these quantities, C_n^2 is calculated following (Kohsiek, 1982)

$$C_n^2 = \frac{A_T^2}{T^2} C_T^2 + 2\frac{A_T A_Q}{TQ} C_{TQ} + \frac{A_Q^2}{Q^2} C_Q^2, \qquad (2)$$

$$A_T = -77.49 \frac{p}{T} 10^{-6}, \qquad (3)$$

$$A_Q = -59.00\, Q\, 10^{-6}, \qquad (4)$$

where p is the atmospheric pressure in mbar, T the temperature in K and Q the water vapour density. The coefficients A_T and A_Q depend weakly on the wavelength of the radiation. It is found that the third term in (2) is negligible as compared to the other two, and that the ratio of the second term to the first one is approximately 0.05/B, where B is the Bowen ratio. Typical values of B > 0.5 are observed, so the second term is 10% or less contributing to C_n^2.

3. Results and discussion

We will present results from two data sets. Set I is from 27 April to 13 May 1988 and set II from 6 September to 23 September 1988. Only for set II in-situ measurements of the structure parameters

are available. For this set, results are presented regarding:

(i) the in-situ temperature structure parameter observed from different time delays;

(ii) a comparison of C_n^2 observed with the scintillometer and C_n^2 following from the in-situ measurements of C_T^2 and C_{TQ};

(iii) the Monin-Obukhov scaling of C_T^2.

For the sets I and II heat fluxes were calculated from the scintillometer observations and compared with in-situ observed heat fluxes. All data presented here are half-hour averages.

(i) <u>In-situ observations of the temperature structure parameter</u>

We define:

$$C^2_{T,\tau_i} = \frac{\left\langle \left[T(t) - T(t+\tau_i) \right]^2 \right\rangle}{\left(U\tau_i \right)^{2/3}}, \qquad (5)$$

where τ_i is a time delay (here: $\tau_1 = 0.08$ s, $\tau_2 = 0.16$ s and $\tau_4 = 0.32$ s), the $< >$ brackets indicate a time average (here, half hour average), and U is the mean wind speed. Figures 3 and 4 present scatterplots of the three structure parameters C_{T1}^2, C_{T1}^2 and C_{T4}^2. It is seen that C_{T1}^2 and C_{T2}^2 compare reasonably well, whereas C_{T4}^2 tends to be less that C_{T1}^2. It would indicate that the distance $U\tau_4$ may be too close to the low wave number end of the inertial subrange. To give an idea: at U = 3 ms^{-1}, $U\tau_4 \approx 1$ m. We do not have temperature spectra available, however, to compare with. In the subsequent calculation of C_n^2 we averaged the three values of C_T^2 and rejected cases with C_{T4}^2/C_{T1}^2 less than 0.7 or larger than 1.4.

(ii) <u>Comparison of C_n^2</u>

In-situ values of C_n^2 were calculated with Eq. (2), neglecting the contribution of C_Q^2:

$$C_n^2 = \frac{A_T^2}{T^2} C_T^2 + 2 \frac{A_T A_Q}{TQ} C_{TQ}. \qquad (6)$$

Observations of C_T^2 and C_{TQ} were used with the above mentioned restriction to C_{T4}^2/C_{T1}^2. Further selection criteria were: wind speed more that 2 ms^{-1}, net radiation >0, and upwind orientation of the temperature sensor with respect to its mount. Fig. 5 shows that on the average the optical C_n^2 compares well with the in-situ C_n^2. However, we should recall that the optical C_n^2 is observed at 23 m height, whereas the in-situ one at 18 m. In first approximation $C_n^2 \sim z^{-1}$, thus one should expect a 18/23 = 0.78 ratio. It may be that for this particular set of data, the displacement height at the tower is less than assumed. The wind direction was almost exclusively between South and South-West, and in that direction the terrain is going down. Thus, turbulent structures may be blown into lower heights above the surface than the heights they originated from.

(iii) The Monin-Obukhov scaling of C_T^2

In the calculation of the sensible heat flux from C_T^2, one makes use of Monin-Obukhov scaling of the structure parameter. Following Wyngaard et al., 1971,

$$\frac{C_T^2 z^{2/3}}{T_*^2} = f_T(z/L), \tag{7}$$

$$f_T(z/L) = 4.9\left(1 - 7\frac{z}{L}\right)^{-2/3} \qquad L < 0, \tag{8}$$

$$= 4.9\left(1 + 2.75\frac{z}{L}\right) \qquad L > 0. \tag{9}$$

In Fig. 6 observed data pairs of $C_T^2 z^{2/3}/T_*^2$, z/L are plotted, together with the relation given by (7), as well as relation from Thiermann and Grassl (1992) and Chintawongvanich and Olsen (1991). In the Appendix the different expressions for f_T (z/L) are given for $z/L < 0$ as well as $z/L > 0$. The observed dimensionless structure parameters tend to exceed the predictions. In fact, they rather well follow the free convection limit of Eq. (8):

$$f_{Tf}(z/L) = 1.34\,(-z/L)^{-2/3}. \tag{10}$$

A similar tendency was observed earlier by Kohsiek (1982) and Kohsiek and Bosveld (1987), but then over short vegetation. In going through the process of data selection (situations where the temperature sensor was on the lee side of the tower, or on the lee side of its mounting structure were excluded, as well as cases with low wind speed (less than 2.5 ms^{-1}) or within half an hour of the moment of change of stability), it was noticed that all rejected observations exaggerate the value of the normalized structure parameter. This may suggest that also the accepted data could be contaminated. Is it that under "perfect" observation conditions the dimensionless structure parameter follows Wyngaard's prediction, but that in less favourable situations, be it in the sense of sensor contamination or in the sense of lack of atmospheric stationarity, the structure parameter apparently is too large? It may explain the irregular behaviour at near-neutral atmospheric stability that were observed at several occasions (Kohsiek and Bosveld, 1987).

Observations of the dimensionless temperature structure parameter for stable atmospheric stability are presented in Fig. 7, together with three functions from the literature. Appreciable discrepancies are noted. Our data fall below these functions, and hardly show any trend with z/L. Is it because in stable situations the atmosphere is even more frequently remote from stationarity than in slightly unstable situations? At present, we can only hypothesize.

The dimensionless water vapour structure parameter follows Wyngaard's function a bit better for $z/L < 0$ than C_T^2 does (Fig. 8). For $z/L > 0$, we have too little observations to be presented. The same also holds for C_{TQ} at all stabilities.

We next look at the sensible heat flux calculated from the refractive index structure parameter (scintillometer), and compare it with sensible heat flux measured with eddy correlation. The data discussed here are sets I and II. Equation (2) may be written as:

$$C_n^2 = \frac{A_T^2}{T^2} C_T^2 \left(1 + \frac{0.05}{B}\right) . \qquad (11)$$

If we insert Eq. (11) in Eq. (7), and we use the free convection form of f_T, Eq. (10), an expression for Q_o results:

$$Q_o = 0.55\, z \left(\frac{g}{T}\right)^{1/2} \left[\frac{T^2}{A_T^2} C_n^2 \Big/ \left(1 + \frac{0.05}{B}\right)\right]^{3/4} . \qquad (12)$$

We put z = 23 m. A_T is given by Eq. (3) with p = 1013 mbar, and B is the Bowen ratio from the eddy correlation measurements. As discussed above, free convection behaviour of C_T^2 is observed even for small values of -z/L. Fig. 9 shows that the scintillation heat flux is less than the eddy correlation flux if -z/L > 0.15. In a way this is surprising, because in particular at large values of Q_o the assumption of free convection would hold true. It was found that the disagreeing observations are mainly from set I the period of late April to early May (see Fig. 10 and 11). In this period of time, the deciduous trees still have to unfold their leaves, and the foliage distribution along the optical path is very inhomogeneous - a mix of evergreens and deciduous trees. It could be that in such a situation the displacement height is far less than 2/3 times the tree tops, and consequently the effective height of the optical path much more than 23 m. For instance, if z = 30 m, there would be a much better agreement for $Q_o > 0.15$ K ms^{-1}.
When the atmosphere is stable, θ_* can be calculated directly from C_T^2:

$$\frac{C_T^2 z^{2/3}}{\theta_*^2} = 6 , \qquad (13)$$

see Fig. 7. C_T^2 in turn was calculated from C_n^2 with

$$C_T^2 = \frac{C_n^2 10^{14}}{94} , \qquad (14)$$

which follows from (2) assuming T = 284 K, p = 1013 mbar and Bowen ratio zero (that means, $C_{TQ} = 0$). Again, z = 23 m was used. The results are depicted in Fig. 12, which shows that the scintillation θ_* is higher than the in-situ θ_*, suggesting that the constant in Eq. (13) is too small. It is less likely that the height z is too large. In Fig. 13 the heat fluxes are shown, obtained by multiplying both θ_*'s with the same u_*. If the scintillation method is considered for the practical

measurement of heat flux under stable conditions, then an additional measurement of u_* is needed - in contrast to the (very) unstable situation, where C_T^2 alone is sufficient.

Conclusion

In deriving the sensible heat flux from scintillation measurements, knowledge of the height of the optical path above the displacement height is needed. At many places in this study poor knowledge of the displacement height turned out to be the main limitation in evaluating how successful the method is. In-situ observations of C_n^2 were found to be about 20% larger than scintillation observations. This comparison was made in September, when the deciduous trees were still fully leaved. A comparison of the (positive) heat flux, calculated from the scintillation observations with the in-situ observations showed a discrepancy of up to a factor of two for the observations made in April-May, when the deciduous trees still had to unfold their leaves. It suggests that in that period of time the displacement height experienced by the scintillation phenomenon is appreciably lower than here assumed. When the atmosphere is stable, the scintillation measurement provides some measure for θ_*. Even more important than the uncertainty on the displacement height, is here the lack of knowledge on the behaviour of the dimensionless temperature structure parameter with stability. When the atmosphere is unstable, the temperature structure parameter seems to follow free convection scaling down to near-neutral stability. However, this may be occasioned by a fortuitous combinations of the "true" behaviour (a levelling off going to neutral) and contamination by instrumental deficiencies and atmospheric non-stationarity (which have the effect of boosting the structure parameter). Such uncertainties make that the comparison of the associated heat fluxes measured by scintillation with in-situ observed fluxes is of limited value. Unfortunately, the atmosphere at say 10-20 m above the forest seldom approaches the free convection limit, where the behaviour of the temperature structure parameter is less prone to doubt.
It will be clear that in view of these phenomena, the original question put at the beginning of this research: "How well is a local measurement representative for a larger part of the forest?", could not be answered. We suggest that future scintillation measurements over forests will be performed at a greater height above the tree tops. In addition, further attention should be paid to the behaviour of the dimensionless C_T^2 with z/L, in particular for slightly unstable to stable atmospheric stabilities, and for non-homogeneous surfaces.

Acknowledgement

The experiment at Garderen was largely carried out by Mr F.C. Bosveld and Mr J.G. van der Vliet. The Gelderland Provincial Electricity Board (PGEM) kindly permitted us to use the tower at Drie. F.C. Bosveld's comments on the draft of this report are appreciated. Marleen Kaltofen typed the report.

Literature

Bosveld, F.C., 1991: Turbulent exchange coefficients over a Douglas fir forest. KNMI Scientific Reports WR 91-2.

Bosveld, F.C., Bouten, W., Noppert, F., Steingröver, E.G., and Tiktak, A., 1992: The ACIFORN hydrological programme, the water cycle of a Douglas fir forest. Submitted for publication in Annales Geophysicae.

Chintawongvanich, P., and Olsen, R.O., 1991: Remote sensing of atmospheric turbulence. Second Symposium on Lower Tropospheric Profiling: Needs and Technologies. Septembert 10-13, 1991, Boulder, Colorado U.S.A.

Kohsiek, W., 1982: Measuring C_T^2, C_Q^2 and C_{TQ} in the unstable surface layer, and relations to the vertical fluxes of heat and moisture. Boundary-Layer Meteor. 24, 89-107.

Kohsiek, W., 1987: A 15 cm aperture LED scintillometer for C_n^2 and crosswind measurements. KNMI Scientific Reports WR 87-3.

Kohsiek, W., and Bosveld, F.C., 1987: Heat and moisture fluxes and related structure parameters in the unstable atmospheric surface layer over short vegetations. KNMI Scientific Reports WR 87-7.

Thiermann, V., and Grassl, H., 1992: The measurement of turbulent surface layer fluxes by use of bichromatic scintillation. Boundary-Layer Meteor. 58, 367-389.

Wyngaard, J.C., Izumi, Y., and Collins Jr., S.A., 1971: Behavior of the refractive-index-structure parameter near the ground. J. Opt. Soc. Am. 61, 1646-1650.

Legend to the figures

Fig. 1 Situation of the forest "Speuld" near Garderen. In the map, the optical path is indicated. The small lettering refers to vegetation types and the year they were planted. jl = Japanese larch; fs = spruce; gd = pine; dg = Douglas fir; bu = beech.

Fig. 2 Plot of the height of the forest floor above mean sea level, the displacement height, and the height of the optical path, as funcitons of the position along the optical path.

Fig. 3 Scatterplot of the structure parameters C_{T1}^2 and C_{T2}^2. Dataset II.

Fig. 4 Scatterplot of the structure parameters C_{T1}^2 and C_{T4}^2. Dataset II.

Fig. 5 Comparison of the optical C_n^2 with the one derived from in-situ observations. Dataset II.

Fig. 6 Behaviour of observed values of $C_T^2\, z^{2/3}/T_*^2$ with stability z/L for $L < 0$. The drawn lines reflect functions of Wyngaard et al., 1971 (W), Thiermann and Grassl, 1991 (T&G) and Chintawongvanich and Olsen, 1991 (C&O). The dashed line is the free convection limit of Wyngaard et al. (Eq. (10)). Dataset II.

Fig. 7 Observations of $C_T^2\, z^{2/3}/T_*^2$ for $L > 0$. The drawn lines represent functions given by Wyngaard et al., 1971 (W), Thiermann and Grassl, 1991 (T&G) and by Chintawongvanich and Olsen, 1991 (C&O). Dataset II.

Fig. 8 Behaviour of $C_Q^2\, z^{2/3}/2$ with z/L for $L < 0$. The drawn line is from Eq. (8) (Wyngaard et al., 1971). Dataset II.

Fig. 9 Sensible heat flux derived from scintillation measurements ($Q_{o,sc}$) compared with eddy correlation measurements ($Q_{o,ec}$). Datasets I and II.

Fig. 10 As Fig. 9, but for the observations in April-May 1988 only (set II).

Fig. 11 As Fig. 9, but for September 1988 only (set I).

Fig. 12 Comparison of θ_* derived from scintillation measurements ($\theta_{*,sc}$) and eddy correlation measurements ($\theta_{*,ec}$), for $L > 0$. Datasets I and II.

Fig. 13 Comparison of the sensible heat flux derived from scintillation measurements ($Q_{o,sc}$) and from eddy correlation measurements ($Q_{o,ec}$), for $L > 0$. Datasets I and II.

Appendix

Expressions for the function f_T (z/L)

	L < 0	**L > 0**
Wyngaard et al. (1971)	$4.9\left(1 - 7\frac{z}{L}\right)^{-2/3}$	$4.9\left(1 + 2.75\frac{z}{L}\right)$
Thiermann and Grassl (1991)	$6.34\left[1 - 7\frac{z}{L} + 75\left(\frac{z}{L}\right)^2\right]^{-1/3}$	$6.34\left[1 + 7\frac{z}{L} + 20\left(\frac{z}{L}\right)^2\right]^{1/3}$
Chintawongvanich and Olsen (1991)	$7.7\left(1 - 17\frac{z}{L}\right)^{-2/3}$	$7.7\,\frac{1 + 36\frac{z}{L}}{1 + 20\frac{z}{L}}$

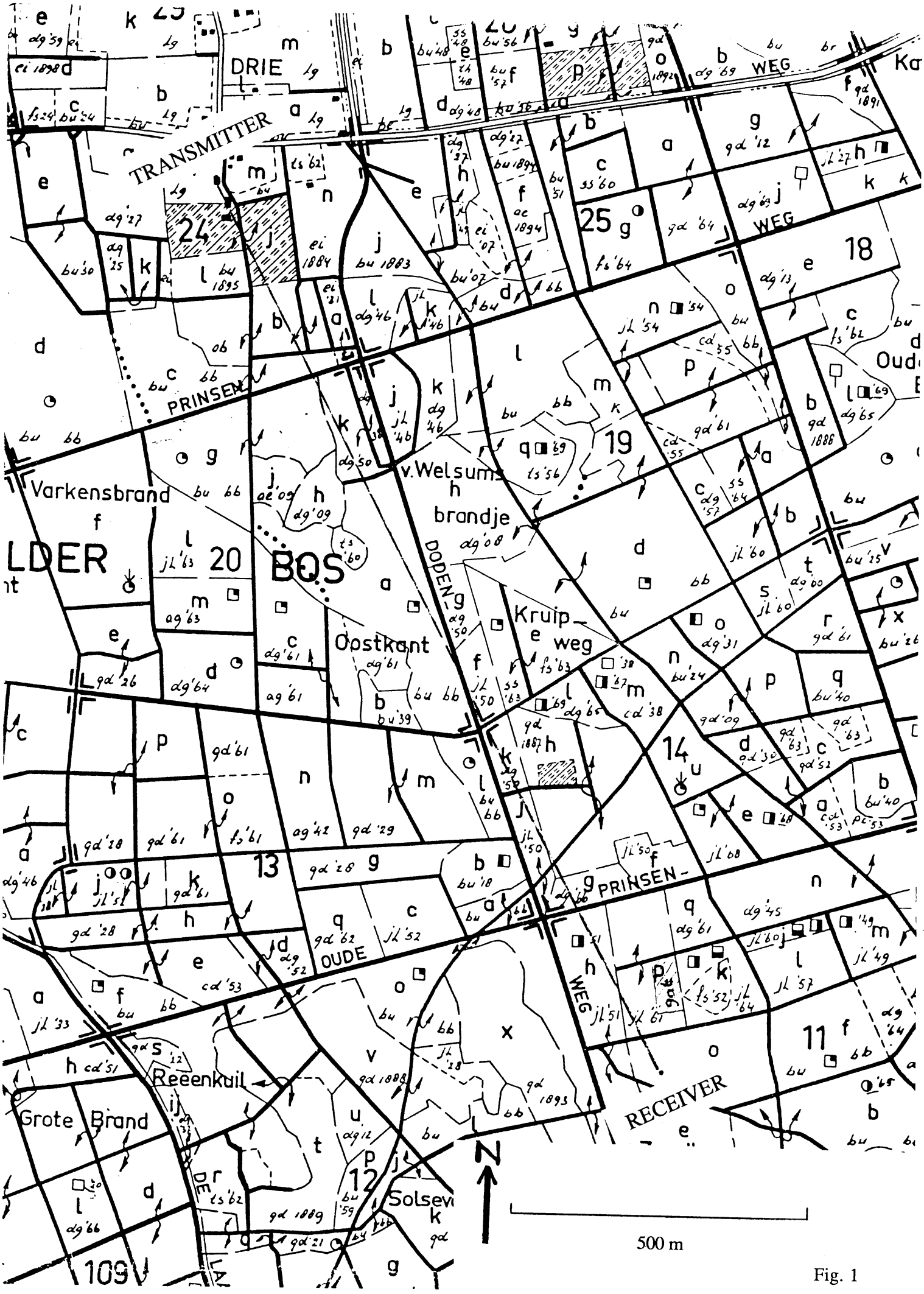
DRIE
TRANSMITTER
WEG
PRINSEN
Varkensbrand
v. Welsums
brandje
DODEN-
LDER
BOS
Oostkant
Kruip-
e weg
OUDE
PRINSEN-
WEG
Reeenkuil
Grote Brand
RECEIVER
Solsevi
N
500 m

Fig. 1

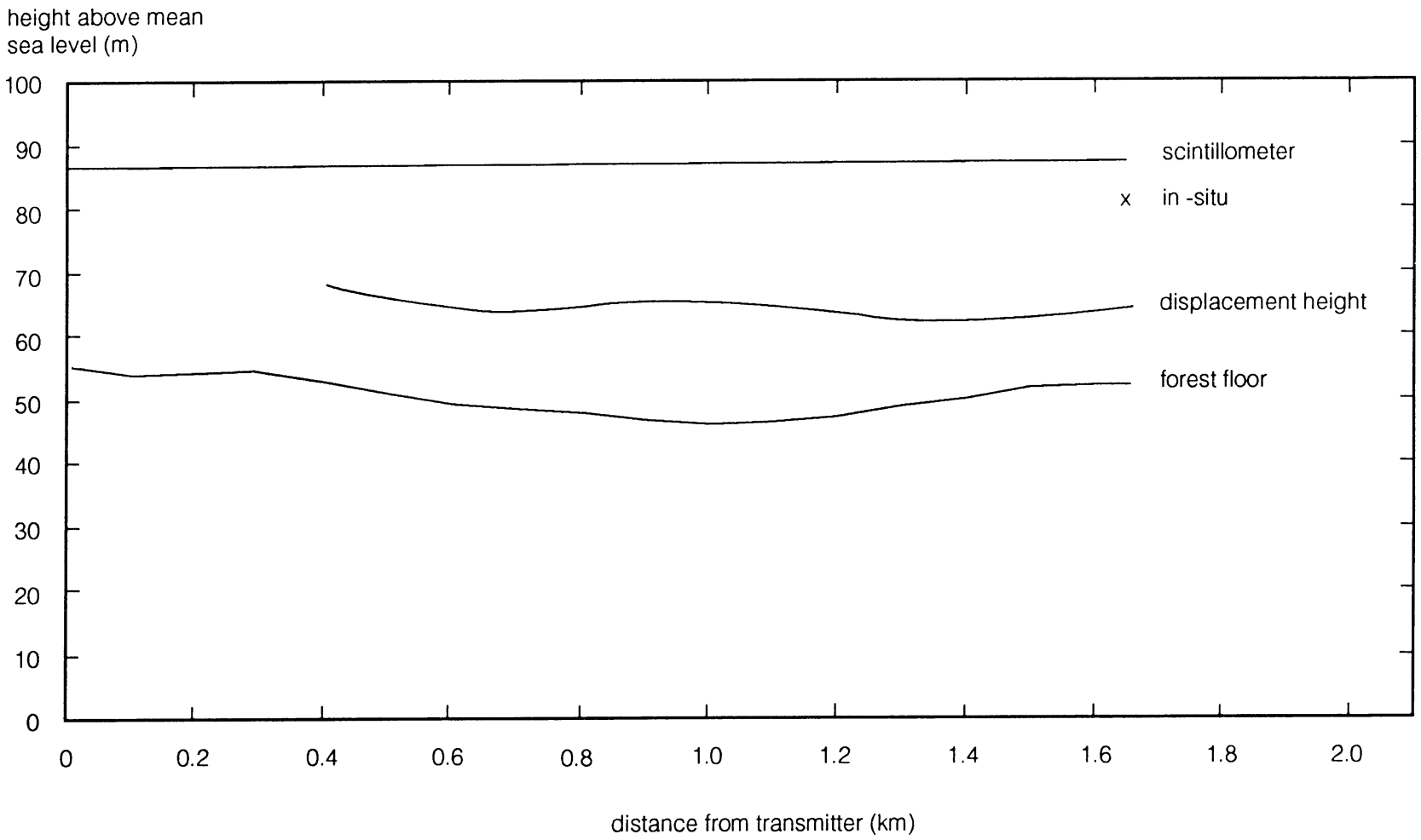
height above mean
sea level (m)
100
90
80
70
60
50
40
30
20
10
0
0
0.2
0.4
0.6
0.8
1.0
1.2
1.4
1.6
1.8
2.0
distance from transmitter (km)
scintillometer
x in -situ
displacement height
forest floor

Fig. 2

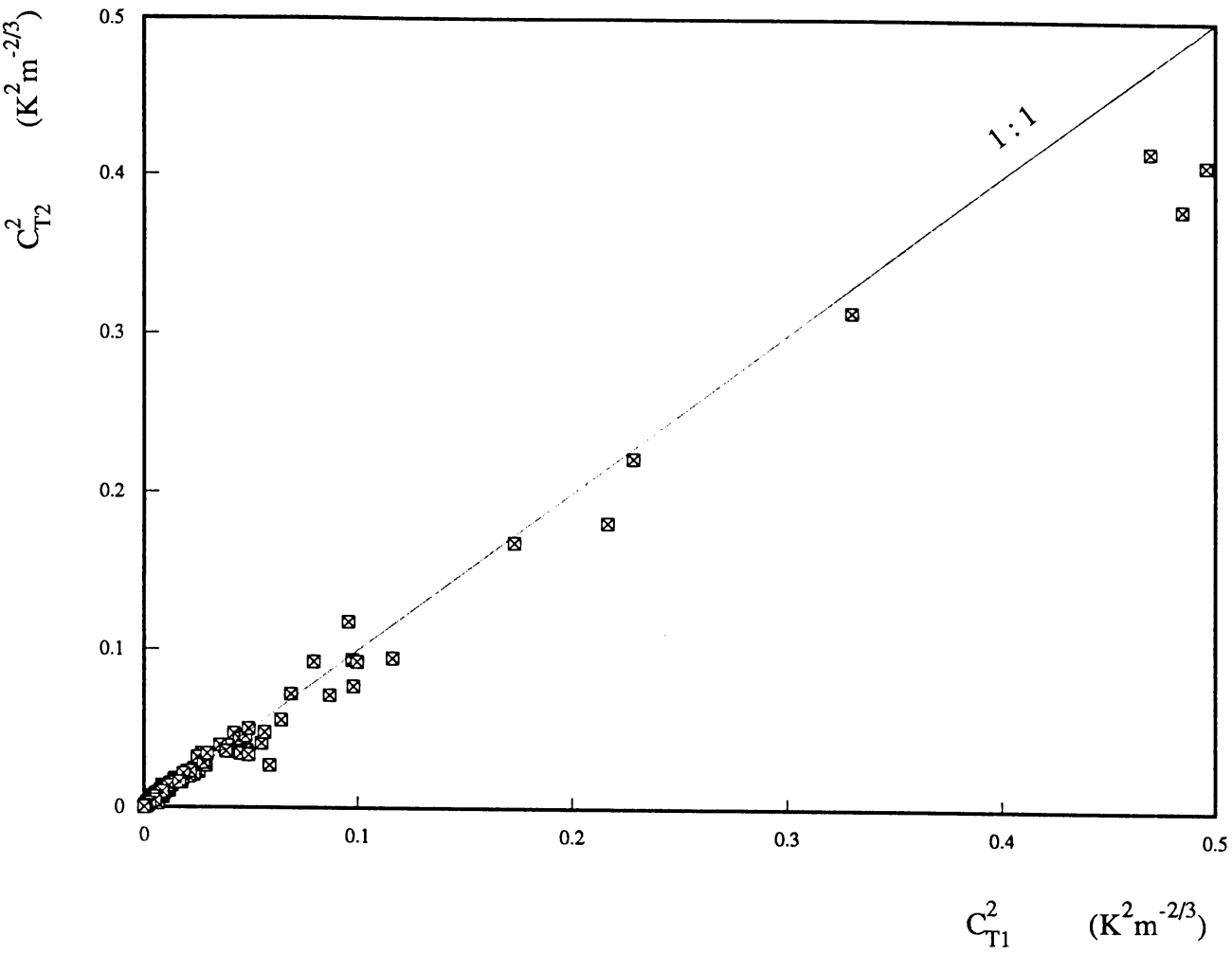

Fig. 3

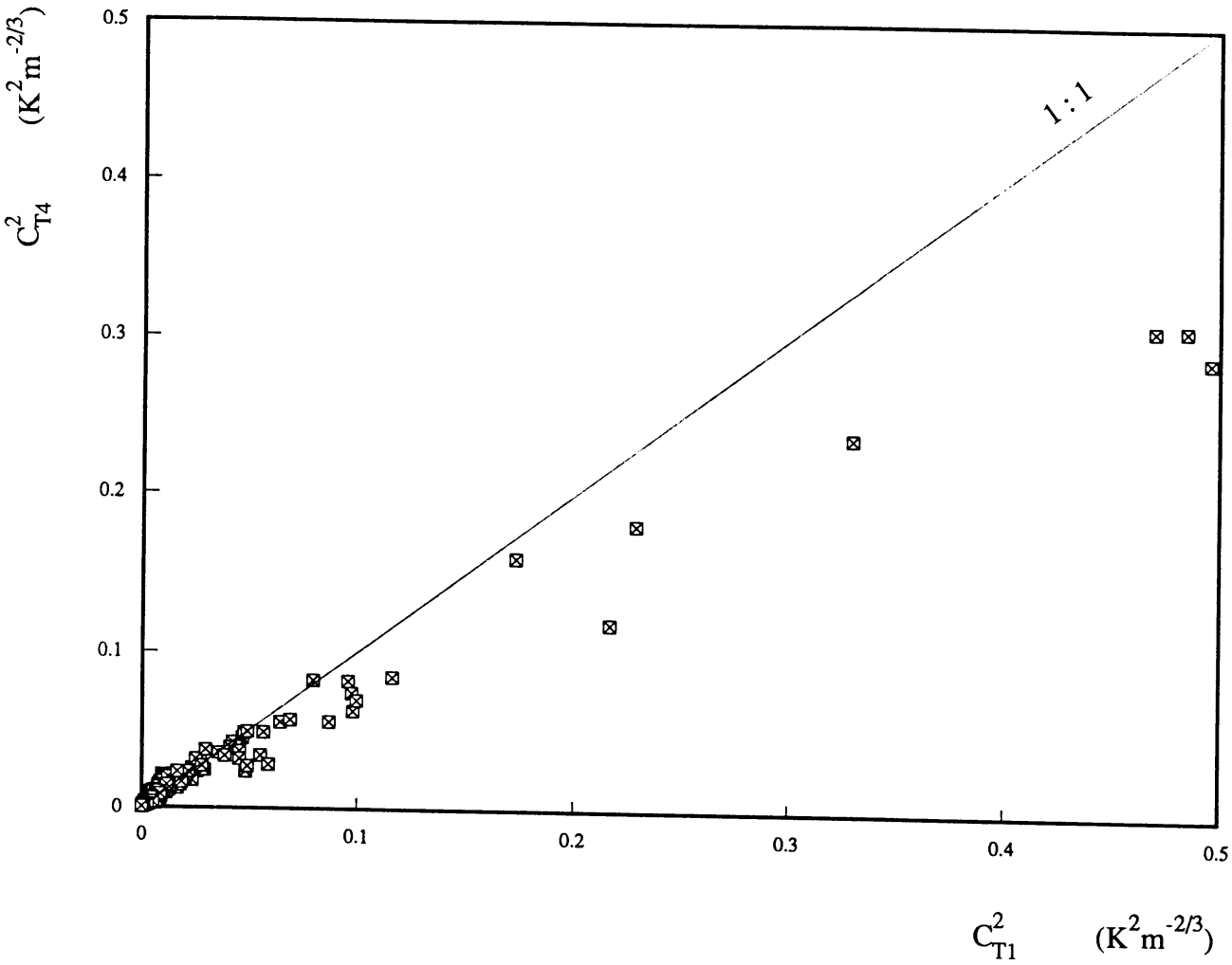

Fig. 4

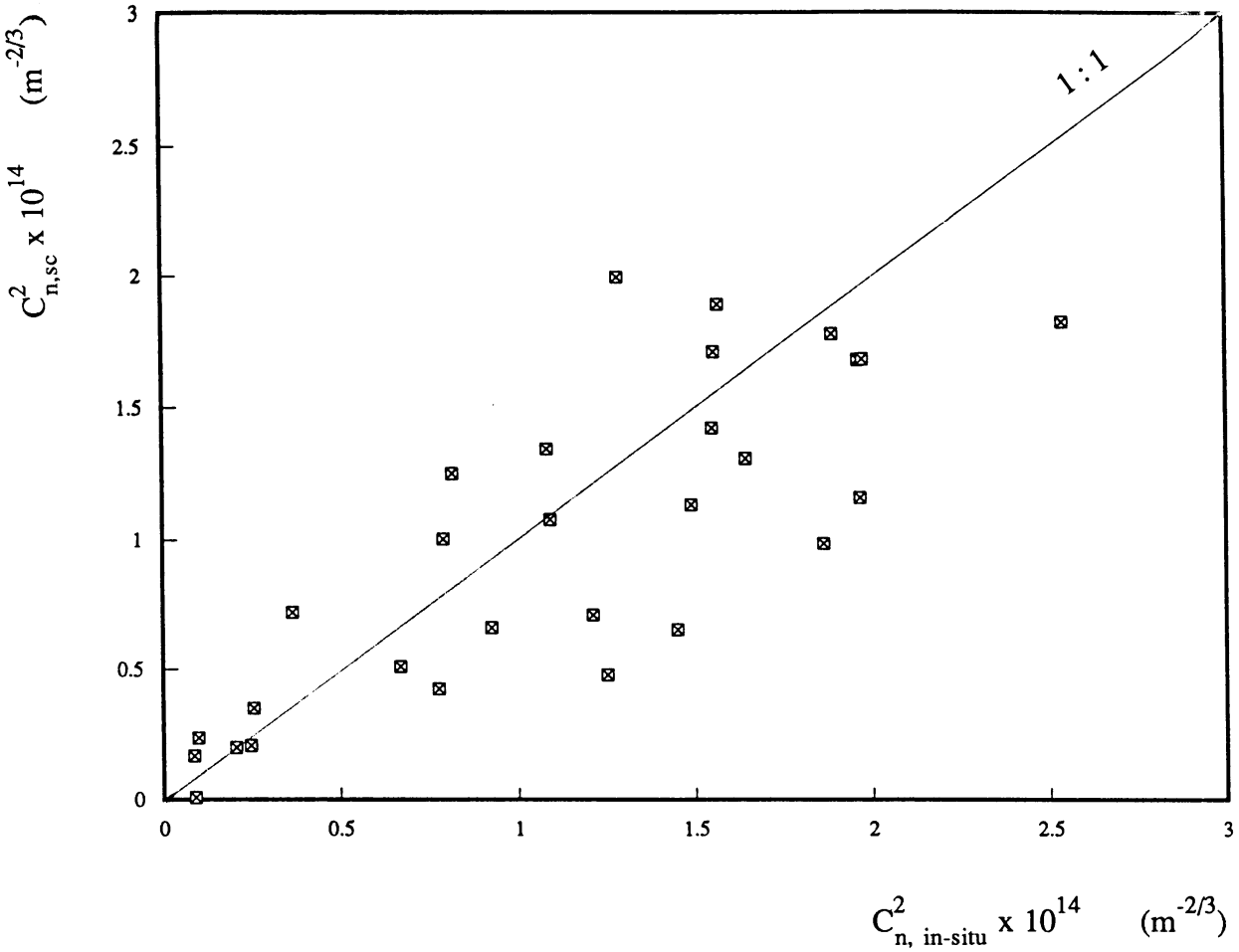

Fig. 5

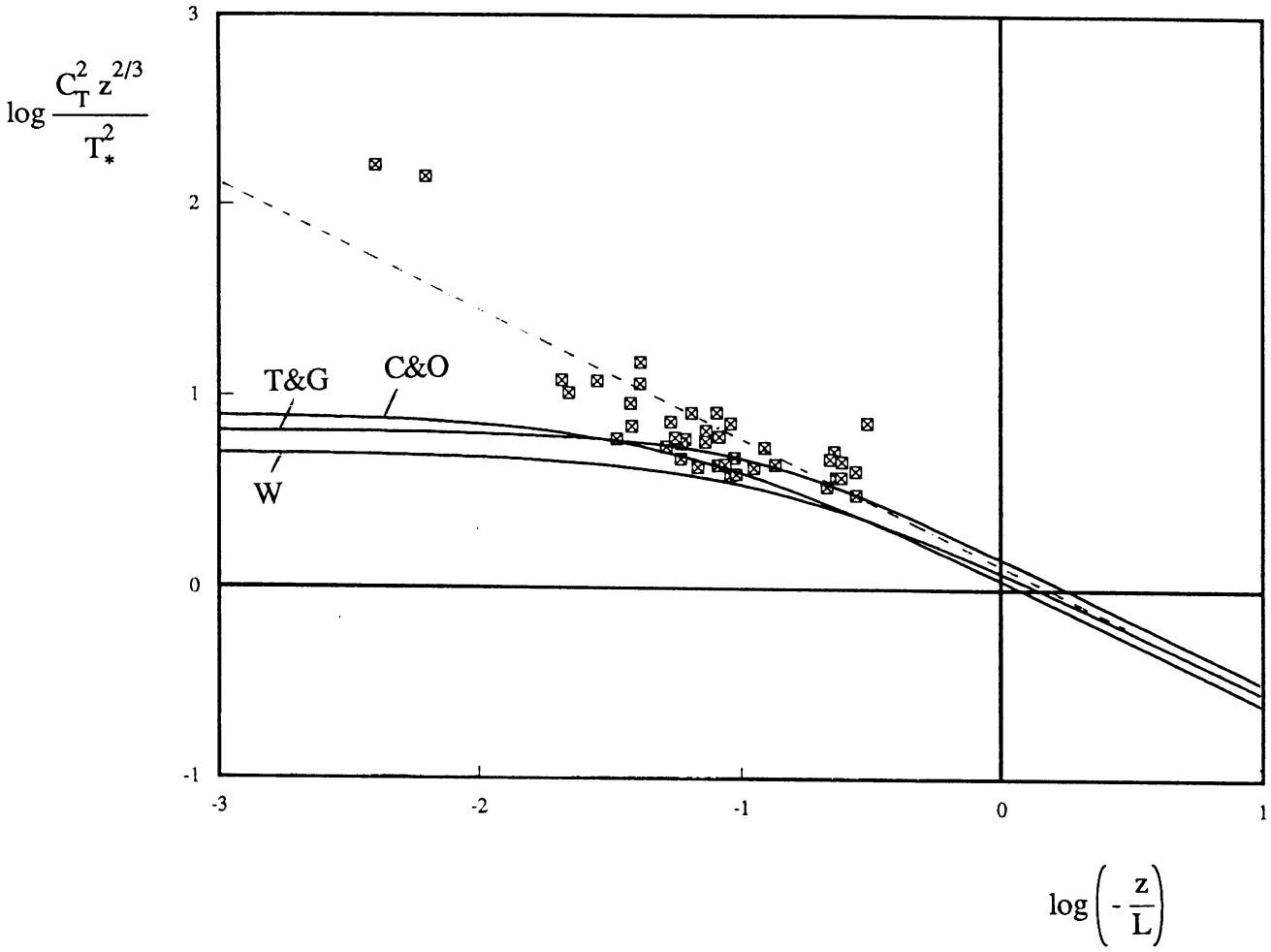

Fig. 6

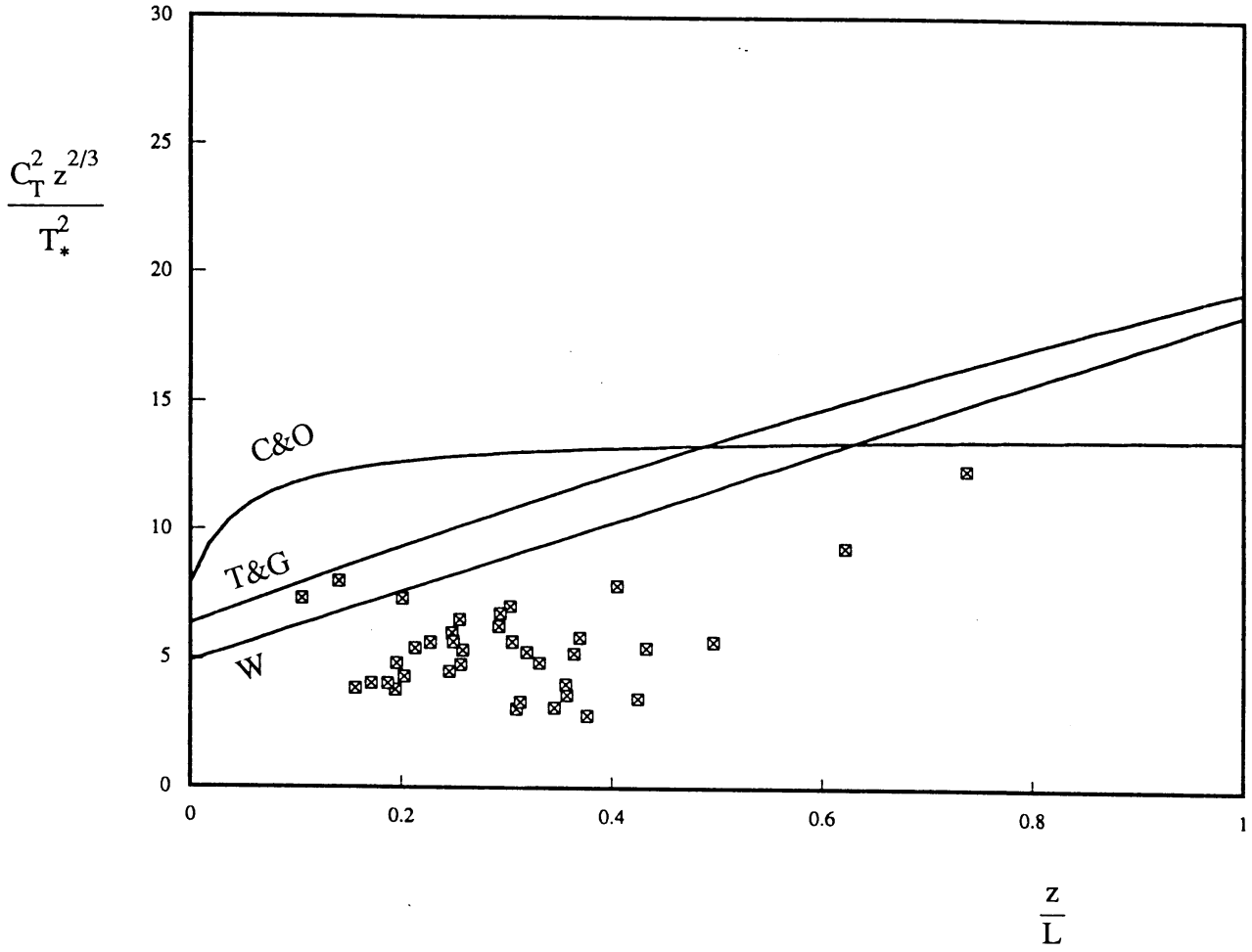

Fig. 7

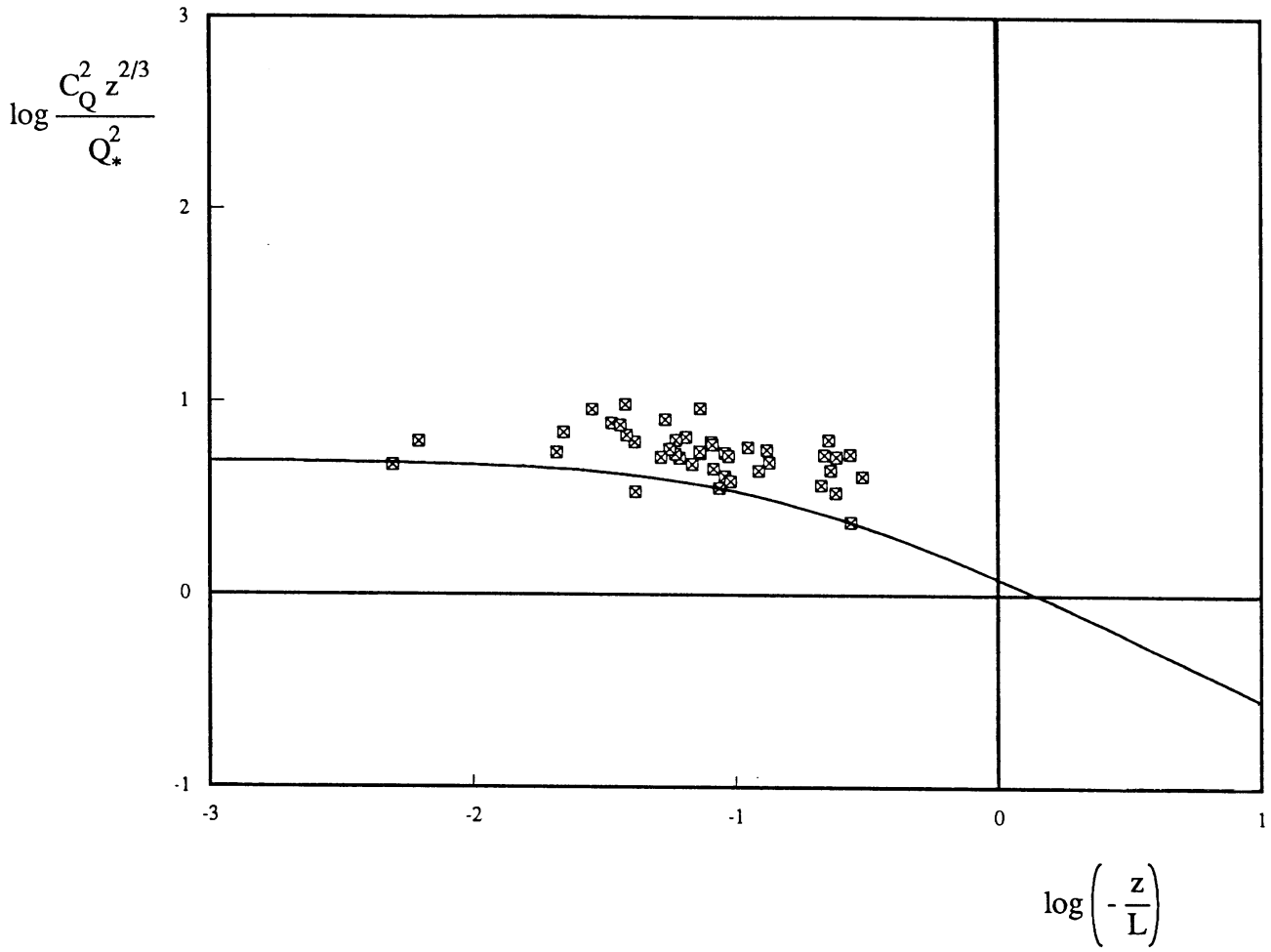

Fig. 8

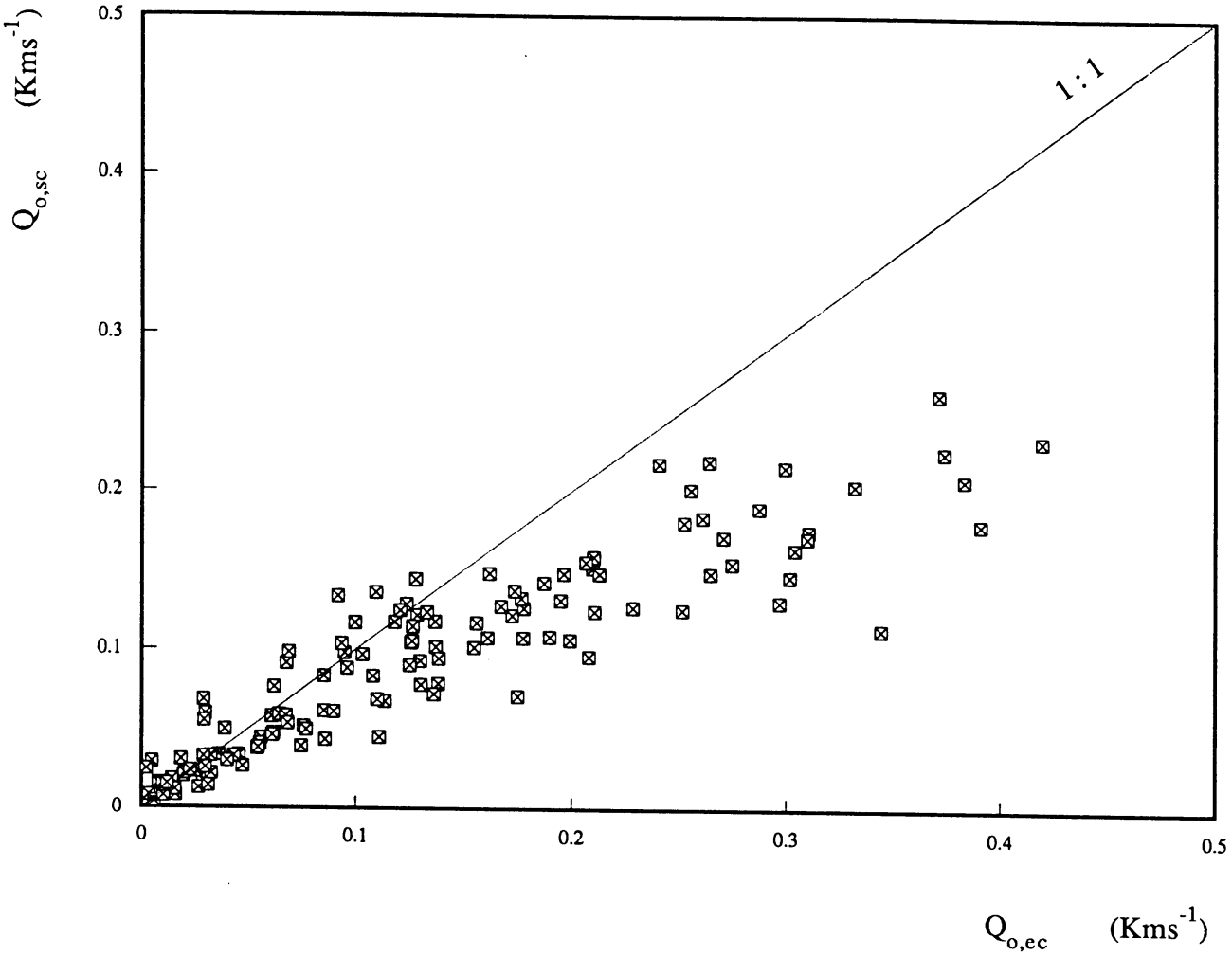

Fig. 9

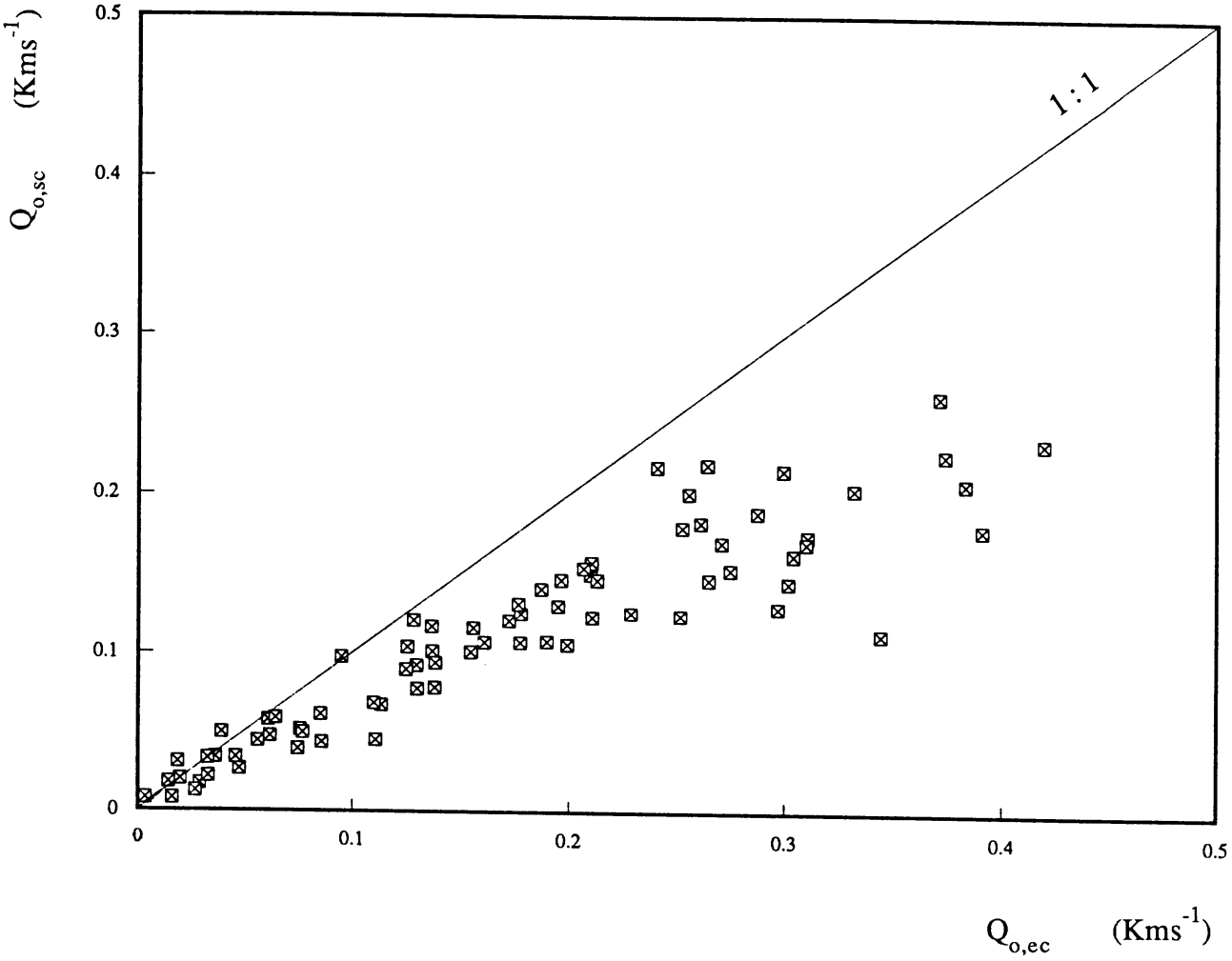

Fig. 10

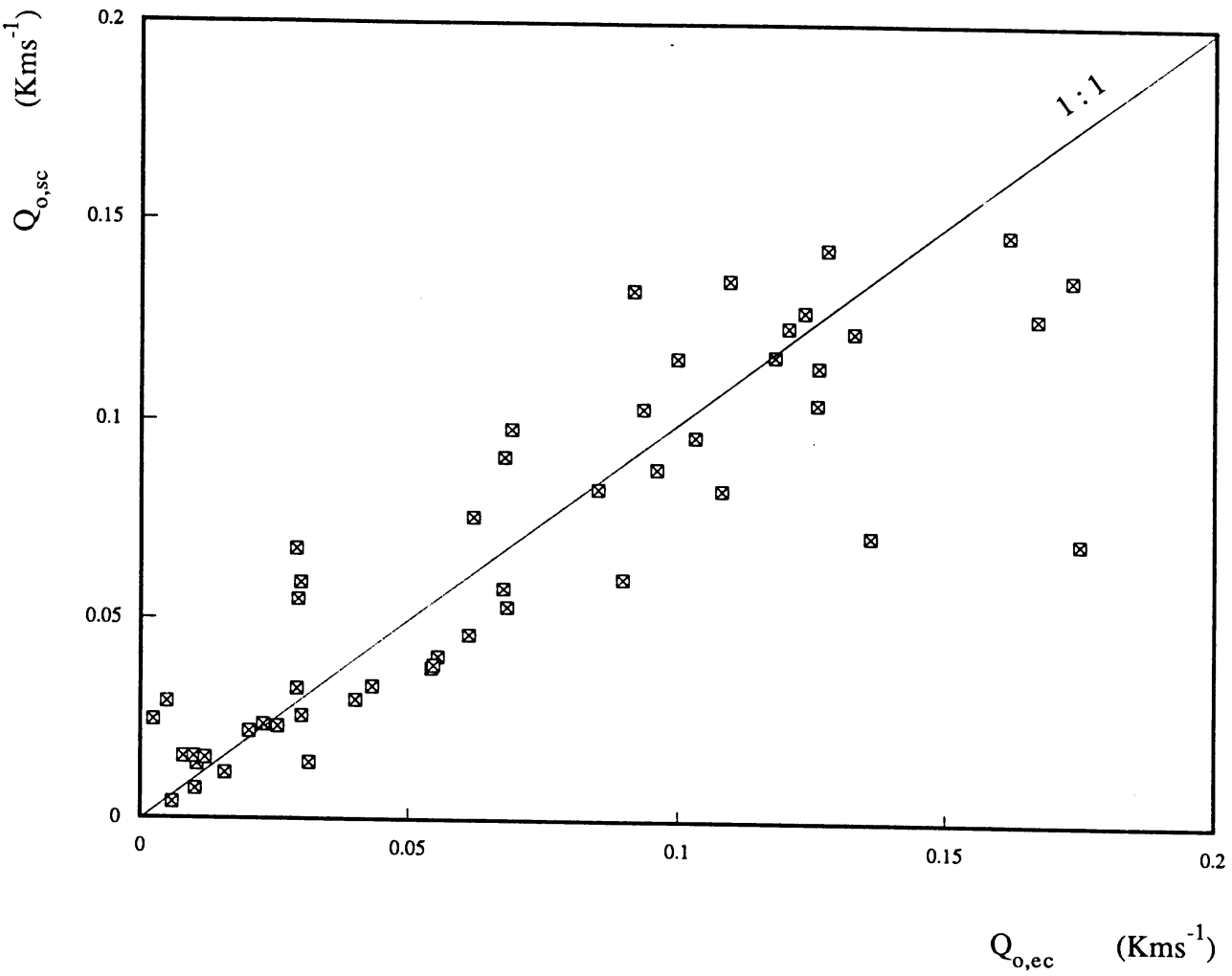

Fig. 11

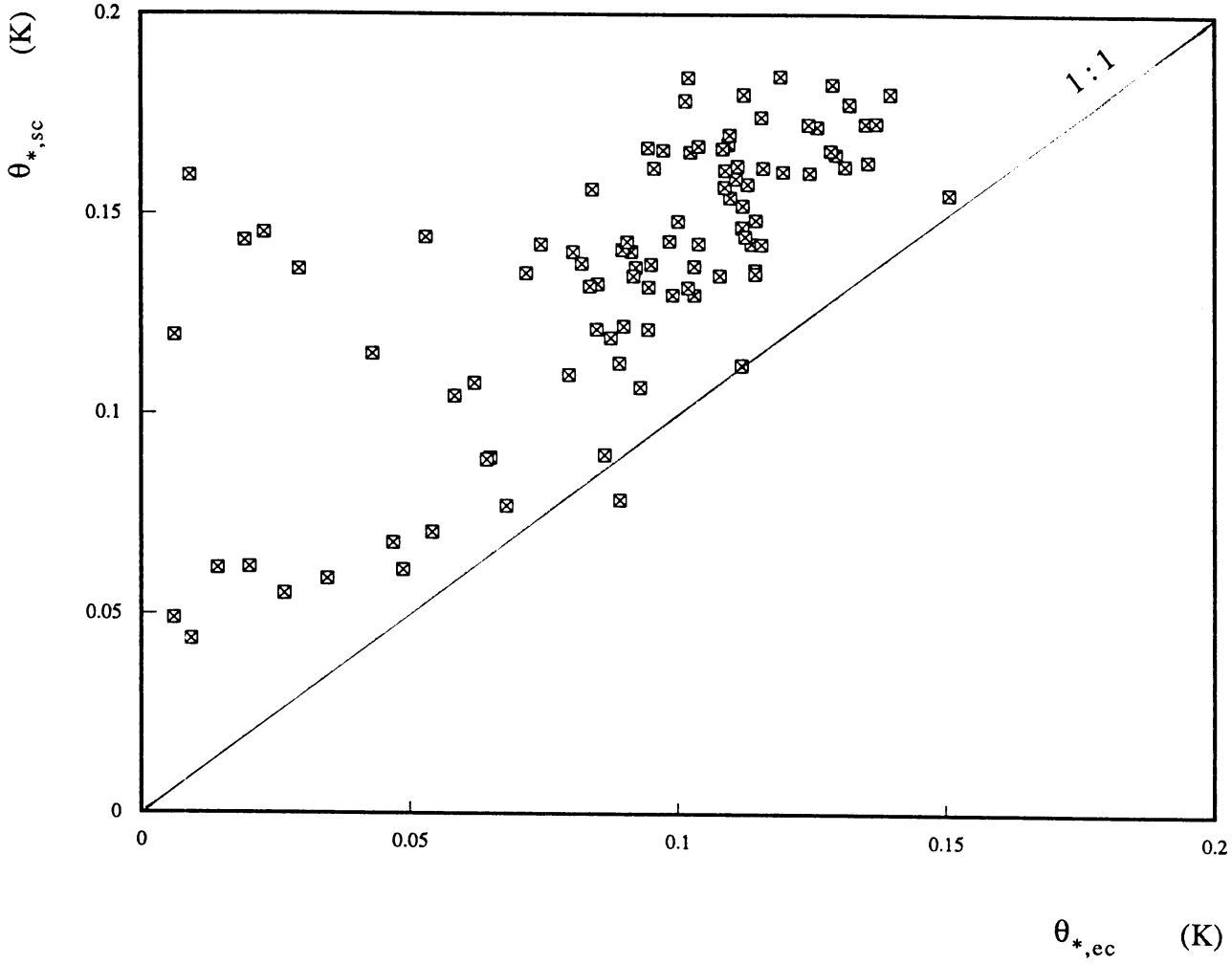

Fig. 12

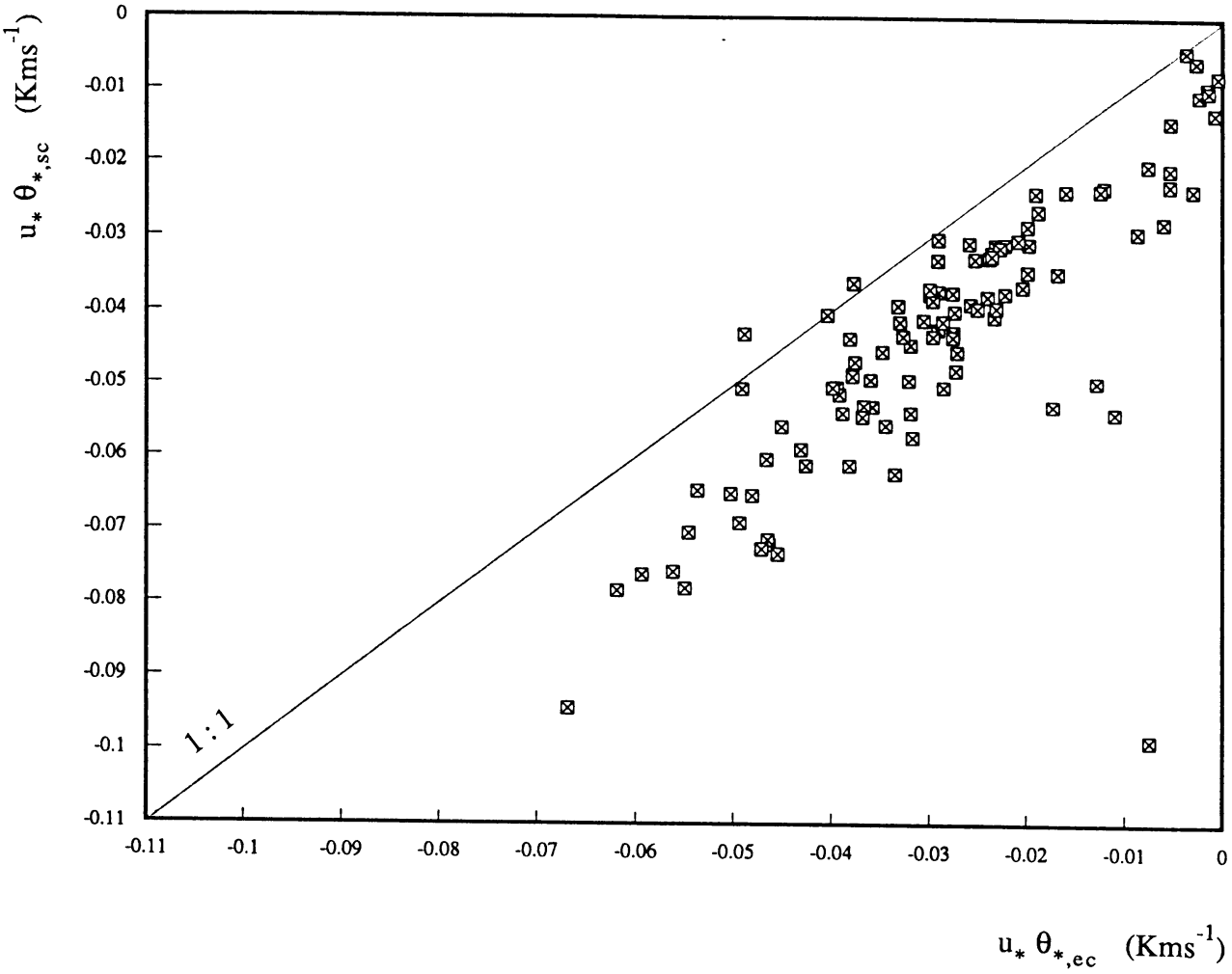
$u_* \theta_{*,sc}$ (Kms^{-1})
0
-0.01
-0.02
-0.03
-0.04
-0.05
-0.06
-0.07
-0.08
-0.09
-0.1
-0.11
1:1
-0.11
-0.1
-0.09
-0.08
-0.07
-0.06
-0.05
-0.04
-0.03
-0.02
-0.01
0
$u_* \theta_{*,ec}$ (Kms^{-1})

Fig. 13